HHS Public Access

Author manuscript

J Am Chem Soc. Author manuscript; available in PMC 2020 February 06.

Published in final edited form as:

J Am Chem Soc. 2019 February 06; 141(5): 1893–1897. doi:10.1021/jacs.8b13094.

A "Clickable" Photoconvertible Small Fluorescent Molecule as a Minimalist Probe for Tracking Individual Biomolecule Complexes

Joomyung V. Jun[†], **Conor M. Haney**[†], **Richard J. Karpowicz Jr.**[$], **Sam Giannakoulias**[†], **Virginia M.-Y. Lee**[$], **E. James Petersson**[†,*], **David M. Chenoweth**[†,*]

[†]Department of Chemistry, University of Pennsylvania, Philadelphia, Pennsylvania 19104, United States

[$]Department of Pathology and Laboratory Medicine, Center for Neurodegenerative Disease Research, University of Pennsylvania, 3600 Spruce Street, Philadelphia, Pennsylvania 19104, United States

Abstract

Photoconvertible fluorophores can enable the visualization and tracking of a specific biomolecules, complexes, and cellular compartments with precise spatiotemporal control. The field of photoconvertible probes is dominated by fluorescent protein variants, which can introduce perturbations to the target biomolecules due to their large size. Here, we present a photoconvertible small molecule, termed CPX, that can be conjugated to any target through azide-alkyne cycloaddition ("click" reaction). To demonstrate its utility, we have applied CPX to study 1) trafficking of biologically relevant synthetic vesicles and 2) intracellular processes involved in transmission of α-synuclein (αS) pathology. Our results demonstrate that CPX can serve as a minimally perturbing probe for tracking the dynamics of biomolecules.

Graphical Abstract

[*]**Corresponding Author** E. James Petersson: ejpetersson@sas.upenn.edu, David M. Chenoweth: dcheno@sas.upenn.edu.

Present Addresses

Conor M. Haney Present Address: 601 S College Road, Wilmington, NC 28403. haneyc@uncw.edu

ASSOCIATED CONTENT

Supporting Information.

The Supporting Information is available free of charge on the ACS Publications website.

Experimental details with supplemental notes, characterization data for new compounds, X-ray structures, and additional live cell fluorescence images (PDF)

The authors declare no competing financial interest.

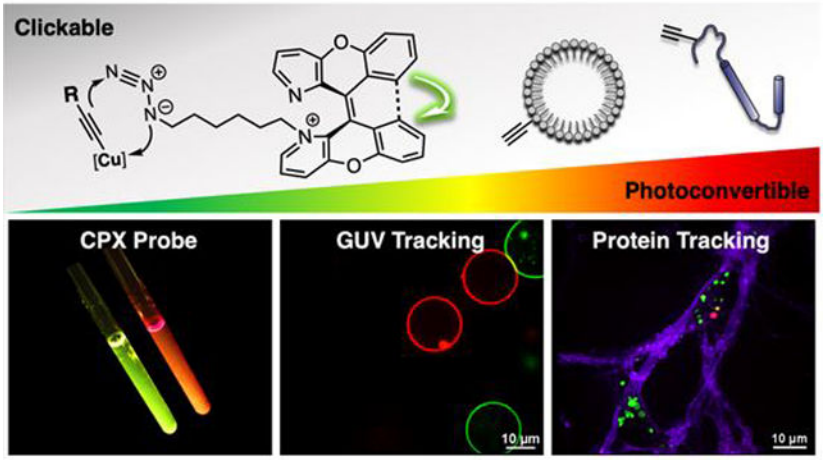

Over the last several decades, there has been a remarkable growth in the number of fluorescence imaging techniques for studying biological systems.[1] Functional fluorescent probes such as photoactivatable fluorophores can provide dynamic information concerning the localization and quantity of biomolecules in living cells.[2–3] Though much progress has been made in recent years with genetically encoded photoactivatable fluorescent proteins (FPs), these are often larger than the target molecule, and can cause undesired aggregation or altered protein function.[2,4–6] Moreover, incorporation of those FPs is generally restricted to the C- or N-terminus, a constraint not optimal for studying dynamic proteins or small targets such as peptides.

A small molecule photoactivatable probe has many potential advantages in terms of size and options for its installation. However, photoactivatable small molecules are still rare and generally depend on “photoactivation,” which refers to the conversion from an initial dark state into a fluorescent state.[2–3,7–9] Recently, the Chenoweth group reported a new class of “photoconvertible” dye built upon a 1,1’-diazaxanthilidene scaffold, that utilizes an activation mechanism based on a photochemically allowed 6π electrocyclization/oxidation reaction leading to the conversion of one fluorescent state to another.[8–10] Unlike other “photoactivation” mechanisms, such as photoisomerization,[11] photouncaging,[12] or photodecomposition of azides,[13] this “photoconvertible” mechanism facilitates visualization of both the pre- and post-activation forms and without producing potentially harmful side products (e.g. nitrosoaromatics) or reactive intermediates (e.g. nitrene). Herein, we present a Clickable and Photoconvertible diazaXanthilidene (CPX) probe made by introducing an orthogonal “clickable” linker to a diazaxanthilidene fluorophore (Figure 1). We demonstrate the advantageous properties of this new CPX probe in two biologically relevant systems, one with phospholipid vesicles and a second with an amyloidogenic protein.

Design and Synthesis of CPX Probe.

Our clickable photoconvertible small molecule fluorescent probe is well-suited for tracking or monitoring biomolecules. In an effort to develop a noninvasive tracking probe, we carefully designed the probe to meet four key criteria: 1) small molecular size (<500 Da) to preserve its non-invasive and minimally perturbing nature (i.e., noncytotoxic for lengthy

analysis), 2) high sensitivity, to visualize biological compounds at physiological concentrations (<μM), 3) efficient photoconversion using mild activating conditions (i.e., visible light), and 4) applicability to versatile targets for widespread use in cell biology.

Recently, we showed that N-methylation of compound **1** (**Me-1**) led to a highly water-soluble, non-cytotoxic, cell-permeable, and readily photoconvertible mitochondria-specific imaging dye.[14] In order to expand the application of **1**, we designed the CPX probe to have a linker with a "clickable" handle that is capable of versatile covalent labeling.[15] The linker was conveniently installed via alkylation of the diazaxanthilidene pyridine nitrogen, rendering the probe water-soluble.[14] The alkane linker length was kept to greater than 3 carbons (3C) to avoid interactions between diazaxanthilidene and azide, which could change the photophysical properties of the fluorophore or reduce the reactivity of the azide. The linker was kept shorter than 7C to avoid generating lipid-like properties, which could decrease solubility as well as localization propensity of the CPX probe. Hence, we investigated CPX probes with linker lengths of 4 carbons and 6 carbons.

Compound **1** was alkylated with diiodohexane or diiodobutane to afford the desired mono-alkylated product **2a** or **2b** in 98% and 88% yields, respectively.[14,16] The reaction was efficiently driven by adding an excess of alkylating agent under refluxing conditions at 90 °C, wherein product formation can be monitored via appearance of a purple color due to generated iodine and triiodide. Simple extraction with hexane and acetonitrile removes excess alkylating agent. The resulting crude reaction can be carried forward directly to the azidation, providing **3a** and **3b** in 99% yield. (Figure 2).

Single crystals of *(Z)*-**2a** were obtained by slow evaporation of acetonitrile to show that *(Z)*-**2a** adopts an anti-folded conformation even with the increased steric hindrance from the 6C linker (Figure 2). The anti-folded conformation and Z-isomer are important requirements for photochemical reaction through a preorganized structure for conrotatory cyclization.[14] Therefore, the *(Z)*-**2a** crystal structure supported our hypothesis that CPX with a 4C or greater linker can preserve the structure allowing photoconvertibility and a flexible reactive handle.

Photophysical properties, including photoconvertibility of **3a**,**3b**, did not show any significant deviation from those of **Me-1** (Figure S16–17). These validations confirmed that the linker does not disrupt the core fluorophore structure. We focused on probe **3a** to demonstrate the utility of the CPX probe. To promote the photocyclization of **3a** in an *in vitro* system, we irradiated **3a** at 420 nm using a Rayonet photoreactor to yield photoconverted (PC) product **3a-PC** in a 42% isolated yield. Gratifyingly, the azide remained intact and did not photodegrade during irradiation (Figure S9). This allows one to vary the order of the click reaction and photoconversion for other applications.

Photoactivation followed by tracking experiments in a confocal microscope were performed using three channels (Figure S18). The pre-activated **3a** was imaged with a 405 nm laser and FITC emission filter (525±18 nm), here referred to as the green channel (405ex/FITC). Photoactivation was achieved by digital-micromirror device (DMD) module, which allows freely customized shape and size for irradiating regions of interest, and a stimulation laser at

440 nm. The post-activated **3a-PC** was excited with 488 nm and/or 561 nm lasers and observed with a Cy5 emission filter (700±36 nm), referred to here as the red channels (488ex/Cy5 and 561ex/Cy5). Merged images of green and red channels were used to investigate the photoconversion of **3a**. The decrease in brightness of "green" and the increase in "red" allows good signal detection of the photoactivated **3a-PC** over background in a spatially defined manner. The remaining "green" serves as a reference background for un-activated regions. To investigate spatially selective photoactivation followed by tracking, regional photo-irradiation was carried out with a dense population of vesicles or live cells.

Photoactivation of GUV.

Giant unilamellar vesicles (GUVs) consisting of **3a** functionalized phospholipids were utilized to represent a simple cell membrane system.[17] GUVs were prepared by a standard electroformation method in sucrose solution.[18–22] Each set of GUVs were formulated with commercially available lipids, 1,2-dioleoyl-*sn-glycero*-3-phosphochline (DOPC) and 1,2-dipalmitoyl-*sn-glycero*-3-phosphoethanolamine-N-dibenzocyclooctyl (16:0 DBCO-PE), and **3a** labeled DBCO-PE (**3a**-PE), which was synthesized via a copper-free click reaction between **3a** and dibenzocyclooctyne (Figure S20–21). GUV1s (5:95 DBCO-PE/DOPC) were formulated and labeled *in situ* by incubating with an excess of **3a** for 20 min prior to imaging. Under the green channel, five GUV1s were found (Figure 3A) and one of GUV1 was selectively photoconverted by irradiating with the 440 nm laser for 60 s (Figure 3B–D). To demonstrate trafficking, GUV2s (5:95 **3a**-PE/DOPC) were synthesized to ensure that every vesicle was homogeneously labeled with **3a**. Two free floating GUV2s were photoactivated (Figure 3E–F). After 2 min, non-photoactivated neighboring vesicles appeared, and could be clearly distinguished from previously photoactivated vesicles (Figure 3G–H).

Photoactivation and Tracking of α-Synuclein.

Aggregates of α-synuclein (αS) are a hallmark of Parkinson's disease.[23] While a role for cellular transmission of aggregates has now been clearly established in the spread of pathology, the mechanisms underlying endocytosis of aggregates, intracellular trafficking, and seeding of aggregation in healthy neurons remain largely unknown, partly due to the lack of appropriate probes.[24] The kinetics of αS inclusion growth have been investigated by others using αS tagged with a FP such as mEOS2 (26 kDa)[25] or PS-CFP2 (27 kDa),[26] both approximately twice the size of αS (14kDa) itself. Specifically, FPs have significant limitations in studying αS pre-formed fibrils (pffs) endocytosis as they can disrupt aggregation when attached to the N-terminus and can be proteolyzed when attached to the C-terminus.[27–28] Hence, a small non-perturbing probe that can be placed at internal sites would be a powerful tool to study αS aggregate dynamics. Here, we show that our probe overcomes the limitations of FPs by incorporating CPX (488 Da) at three different positions in the αS protein.

Previously, the Petersson group has developed an efficient way to engineer and purify αS with propargyl tyrosine (PpY) incorporated site-specifically using unnatural amino acid mutagenesis in combination with a traceless C-terminal intein tag (Figure 4A).[29–32] **3a** was

conjugated to αS constructs with PpY (αS-PpY[3a]) at position 94, 114 or 136 (Figure S26–(29). Following purification, the three protein constructs of monomeric αS-PpY[3a] were tested for photoconversion and aggregated to demonstrate that these **3a**-labeled fibrils can be photoconverted over 6 h of irradiation *in vitro* without degradation (Figure 4B–E and Figure S30–S36). As we previously found position 114 to be a non-perturbing location for the attachment of other fluorescent dyes (e.g., BODIPY), the **3a**-labeled αS-Ppy114 pre-formed fibrils (**3a**-pffs) were used to investigate the internalization and endolysosomal trafficking of αS following protocols developed in the Lee laboratory (see Figure S37–S40 for fibril characterizations).[24]

The **3a**-pffs were transduced into 7–10 days old mouse primary hippocampal neurons over a period of 20 h. Prior to imaging, trypan blue was added to stain the neuronal membrane to distinguish internalized **3a**-pffs from extracellular material (Figure 5A). An individual endosome/lysosome with internalized **3a**-pffs was then activated by laser irradiation to enable tracking of the pffs (Figure 5B–C). Sequential photoactivation was achieved with excellent spatial control over individual endosome/lysosome in crowded environments (Figure 5D–O). Trypan blue is false-colored to blue in the 561ex/Cy5 channel (Figure 5E,I,M). The appearance of red vesicles (Figure 5F,J,N) and corresponding disappearance of green vesicles (Figure 5G,K,O) indicated successful photoconversion. Lastly, the tracking of **3a**-pffs for 3 h following photoconversion showed that we can indeed monitor the specific **3a**-pffs (Figure 5P–T, Figure S44–S52). These new tools will enable future studies involving larger populations and specific challenges to endosome integrity (e.g., chloroquine treatment) to further explore αS internalization using **3a**-pffs to determine unusual characteristics of certain vesicles that may lead to pathology.

In conclusion, we have developed a clickable and photoconvertible small molecule fluorescent probe that is based on an electrocyclization/oxidation mechanism.[14] The probe is water-soluble, cell-permeable, non-cytotoxic, and small in size allowing for cellular protein localization and tracking studies with minimal perturbation. The applications demonstrated here show the ability to impart precise spatiotemporal control, even in living cells for lengthy experiments of up to 8 h. Furthermore, **2a**,**2b** is not only a precursor to azides; other molecules ready for bioconjugation can be generated by nucleophilic displacement of the iodide. Another advantage of the technology that we wish to emphasize is that the photophysical properties of a small molecule can be drastically modulated by the inclusion of electron-withdrawing or electron-donating groups,[33] therefore studies are underway to alter the CPX pre- and post-conversion spectra. Beyond the proof-of-principle demonstrations here with αS, CPX will be a valuable probe for measuring and monitoring the movement of individual biomolecules or complexes, which are essential not only for basic biology research but also for the diagnosis and treatment of disease.

Supplementary Material

Refer to Web version on PubMed Central for supplementary material.

ACKNOWLEDGMENT

The authors would like to thank Dr. Mai N. Tran for providing chemicals, Dr. Roy M. Malamakal for helpful discussions regarding synthesis, and Sankalp Shukla for assistance in GUV synthesis. We also thank Dr. Charles W. Ross III (University of Pennsylvania) for assistance in HRMS analysis, Dr. Patrick Carroll (University of Pennsylvania) for X-ray analysis, Dr. Jun Gu (University of Pennsylvania) for NMR assistance, and Anna Steiber for technical assistance with TEM imaging. Lastly, we thank Phuson V. Hulamm, Frank E. Herbert, and Timothy Mullen for setting up Nikon microscope and technical assistance.

Funding Sources

This work was supported by funding from the University of Pennsylvania, by the National Institutes of Health (NIH R56-NS081033 to E.J.P. and R01-GM118510 to D.M.C.). C.M.H was supported by an Age-Related Neurodegenerative Disease Training Grant (NIH T32AG000255). V.M.Y.L was supported by AG053488. Instrument support from the National Institutes of Health (Grant NIH RR- 023444) includes HRMS and MALDI (National Science Foundation MRI 0820996).

References

1. Ueno T; Nagano T, Fluorescent probes for sensing and imaging. Nature Methods 2011, 8, 642. [PubMed: 21799499]
2. Maurel D; Banala S; Laroche T; Johnsson K, Photoactivatable and Photoconvertible Fluorescent Probes for Protein Labeling. ACS Chemical Biology 2010, 5 (5), 507–516. [PubMed: 20218675]
3. Grimm JB; English BP; Choi H; Muthusamy AK; Mehl BP; Dong P; Brown TA; Lippincott-Schwartz J; Liu Z; Lionnet T; Lavis LD, Bright photoactivatable fluorophores for single-molecule imaging. Nature Methods 2016, 13, 985. [PubMed: 27776112]
4. Lukyanov KA; Chudakov DM; Lukyanov S; Verkhusha VV, Photoactivatable fluorescent proteins. Nature Reviews Molecular Cell Biology 2005, 6, 885. [PubMed: 16167053]
5. Tsien RY, The Green Fluorescent Protein. Annual Review of Biochemistry 1998, 67 (1), 509–544.
6. Krasowska J; Olasek M; Bzowska A; Clark PL; Wielgus-Kutrowska B, The comparison of aggregation and folding of enhanced green fluorescent protein (EGFP) by spectroscopic studies. Spectroscopy 2010, 24 (3–4).
7. Carlson AL; Fujisaki J; Wu J; Runnels JM; Turcotte R; Spencer JA; Celso CL; Scadden DT; Strom TB; Lin CP, Correction: Tracking Single Cells in Live Animals Using a Photoconvertible Near-Infrared Cell Membrane Label. PLOS ONE 2013, 8 (11), 10.1371/annotation/c05446df-ee55-4072-940c-543adff42086. Original: 10.1371/journal.pone.0069257
8. Tran MN; Chenoweth DM, Photoelectrocyclization as an Activation Mechanism for Organelle-Specific Live-Cell Imaging Probes. Angewandte Chemie International Edition 2015, 54 (22), 6442–6446. [PubMed: 25950154]
9. Tran MN; Rarig R-AF; Chenoweth DM, Synthesis and properties of lysosome-specific photoactivatable probes for live-cell imaging. Chemical Science 2015, 6 (8), 4508–4512. [PubMed: 28496967]
10. Rarig R-AF; Tran MN; Chenoweth DM, Synthesis and Conformational Dynamics of the Reported Structure of Xylopyridine A. Journal of the American Chemical Society 2013, 135 (24), 9213–9219. [PubMed: 23742249]
11. Guo X; Zhou J; Siegler MA; Bragg AE; Katz HE, Visible-Light-Triggered Molecular Photoswitch Based on Reversible E/Z Isomerization of a 1,2-Dicyanoethene Derivative. Angewandte Chemie International Edition 2015, 54 (16), 4782–4786. [PubMed: 25707025]
12. Gagey N; Neveu P; Benbrahim C; Goetz B; Aujard I; Baudin J-B; Jullien L, Two-Photon Uncaging with Fluorescence Reporting: Evaluation of the o-Hydroxycinnamic Platform. Journal of the American Chemical Society 2007, 129 (32), 9986–9998. [PubMed: 17658803]
13. Lord SJ; Conley NR; Lee H.-l. D.; Samuel R; Liu N; Twieg RJ; Moerner WE A Photoactivatable Push−Pull Fluorophore for Single-Molecule Imaging in Live Cells. Journal of the American Chemical Society 2008, 130 (29), 9204–9205. [PubMed: 18572940]

14. Tran MN; Chenoweth DM, Photoelectrocyclization Turn-On Probe for Organelle Specific Spatiotemporally Defined Live Cell Imaging. Angewandte Chemie (International ed. in English) 2015, 54 (22), 6442–6446. [PubMed: 25950154]
15. Sletten EM; Bertozzi CR, Bioorthogonal Chemistry: Fishing for Selectivity in a Sea of Functionality. Angewandte Chemie International Edition 2009, 48 (38), 6974–6998. [PubMed: 19714693]
16. Kele P; Mezö G; Achatz D; Wolfbeis OS, Dual Labeling of Biomolecules by Using Click Chemistry: A Sequential Approach. Angewandte Chemie International Edition 2008, 48 (2), 344–347.
17. Baykal-Caglar E; Hassan-Zadeh E; Saremi B; Huang J, Preparation of giant unilamellar vesicles from damp lipid film for better lipid compositional uniformity. Biochimica et Biophysica Acta (BBA) - Biomembranes 2012, 1818 (11), 2598–2604. [PubMed: 22652256]
18. Mathivet L; Cribier S; Devaux PF, Shape change and physical properties of giant phospholipid vesicles prepared in the presence of an AC electric field. Biophysical Journal 1996, 70 (3), 1112–1121. [PubMed: 8785271]
19. Tian A; Baumgart T, Sorting of Lipids and Proteins in Membrane Curvature Gradients. Biophysical Journal 2009, 96 (7), 2676–2688. [PubMed: 19348750]
20. Ayuyan AG; Cohen FS, Lipid Peroxides Promote Large Rafts: Effects of Excitation of Probes in Fluorescence Microscopy and Electrochemical Reactions during Vesicle Formation. Biophysical Journal 2006, 91 (6), 2172–2183. [PubMed: 16815906]
21. Angelova MI; Soléau S; Méléard P; Faucon F; Bothorel P In Preparation of giant vesicles by external AC electric fields Kinetics and applications, Trends in Colloid and Interface Science VI, Darmstadt, 1992//; Helm C; Lösche M; Möhwald H, Eds. Steinkopff: Darmstadt, 1992; pp 127–131.
22. Graber ZT; Shi Z; Baumgart T, Cations induce shape remodeling of negatively charged phospholipid membranes. Physical Chemistry Chemical Physics 2017, 19 (23), 15285–15295. [PubMed: 28569910]
23. Lashuel HA; Overk CR; Oueslati A; Masliah E, The many faces of α-synuclein: from structure and toxicity to therapeutic target. Nature Reviews Neuroscience 2012, 14, 38.
24. Karpowicz RJ; Haney CM; Mihaila TS; Sandler RM; Petersson EJ; Lee VM-Y, Selective imaging of internalized proteopathic α-synuclein seeds in primary neurons reveals mechanistic insight into transmission of synucleinopathies. Journal of Biological Chemistry 2017, 292 (32), 13482–13497. [PubMed: 28611062]
25. Fares M-B; Maco B; Oueslati A; Rockenstein E; Ninkina N; Buchman VL; Masliah E; Lashuel HA, Induction of de novo α-synuclein fibrillization in a neuronal model for Parkinson's disease. Proceedings of the National Academy of Sciences 2016, 113 (7), E912.
26. Koga H; Martinez-Vicente M; Macian F; Verkhusha VV; Cuervo AM, A photoconvertible fluorescent reporter to track chaperone-mediated autophagy. Nature communications 2011, 2, 386–386.
27. Li W; West N; Colla E; Pletnikova O; Troncoso JC; Marsh L; Dawson TM; Jäkälä P; Hartmann T; Price DL; Lee MK, Aggregation promoting C-terminal truncation of alpha-synuclein is a normal cellular process and is enhanced by the familial Parkinson's disease-linked mutations. Proceedings of the National Academy of Sciences of the United States of America 2005, 102 (6), 2162–2167. [PubMed: 15684072]
28. Trexler AJ; Rhoades E, Single Molecule Characterization of α-Synuclein in Aggregation-Prone States. Biophysical Journal 2010, 99 (9), 3048–3055. [PubMed: 21044603]
29. Haney CM; Wissner RF; Warner JB; Wang YJ; Ferrie JJ; J. Covell D; Karpowicz RJ; Lee VMY; James Petersson E, Comparison of strategies for non-perturbing labeling of α-synuclein to study amyloidogenesis. Organic & Biomolecular Chemistry 2016, 14 (5), 1584–1592. [PubMed: 26695131]
30. Haney CM; Petersson EJ, Fluorescence spectroscopy reveals N-terminal order in fibrillar forms of α-synuclein. Chemical Communications 2018, 54 (7), 833–836. [PubMed: 29313531]

31. Batjargal S; Walters CR; Petersson EJ, Inteins as Traceless Purification Tags for Unnatural Amino Acid Proteins. Journal of the American Chemical Society 2015, 137 (5), 1734–1737. [PubMed: 25625321]

32. Wang L; Schultz PG, Expanding the Genetic Code. Angewandte Chemie International Edition 2004, 44 (1), 34–66. [PubMed: 15599909]

33. Jun JV; Petersson EJ; Chenoweth DM, Rational Design and Facile Synthesis of a Highly Tunable Quinoline-Based Fluorescent Small-Molecule Scaffold for Live Cell Imaging. Journal of the American Chemical Society 2018, 140 (30), 9486–9493. [PubMed: 30028130]

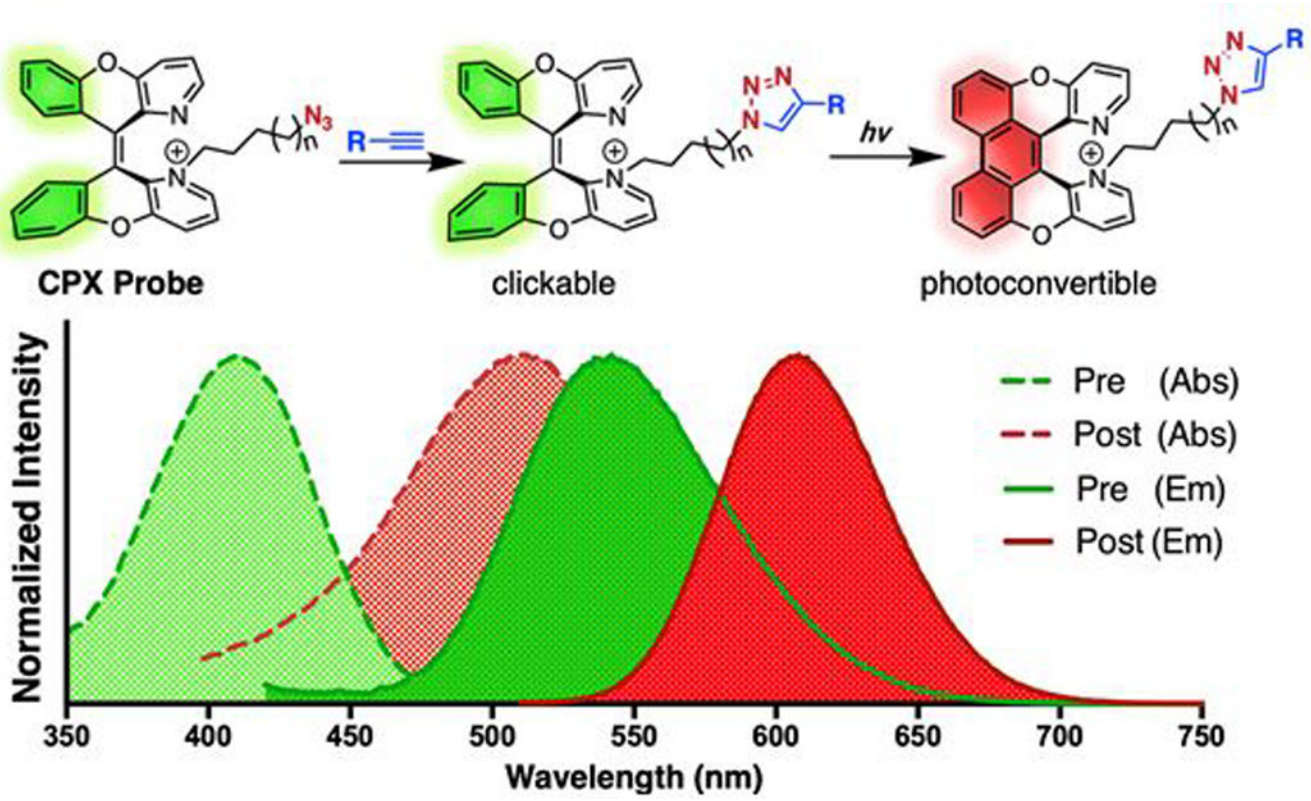

Figure 1.

General structure of CPX probe with absorption (dashed line) and emission (solid line) spectra of pre- (green) and post-activated (red) forms shown.

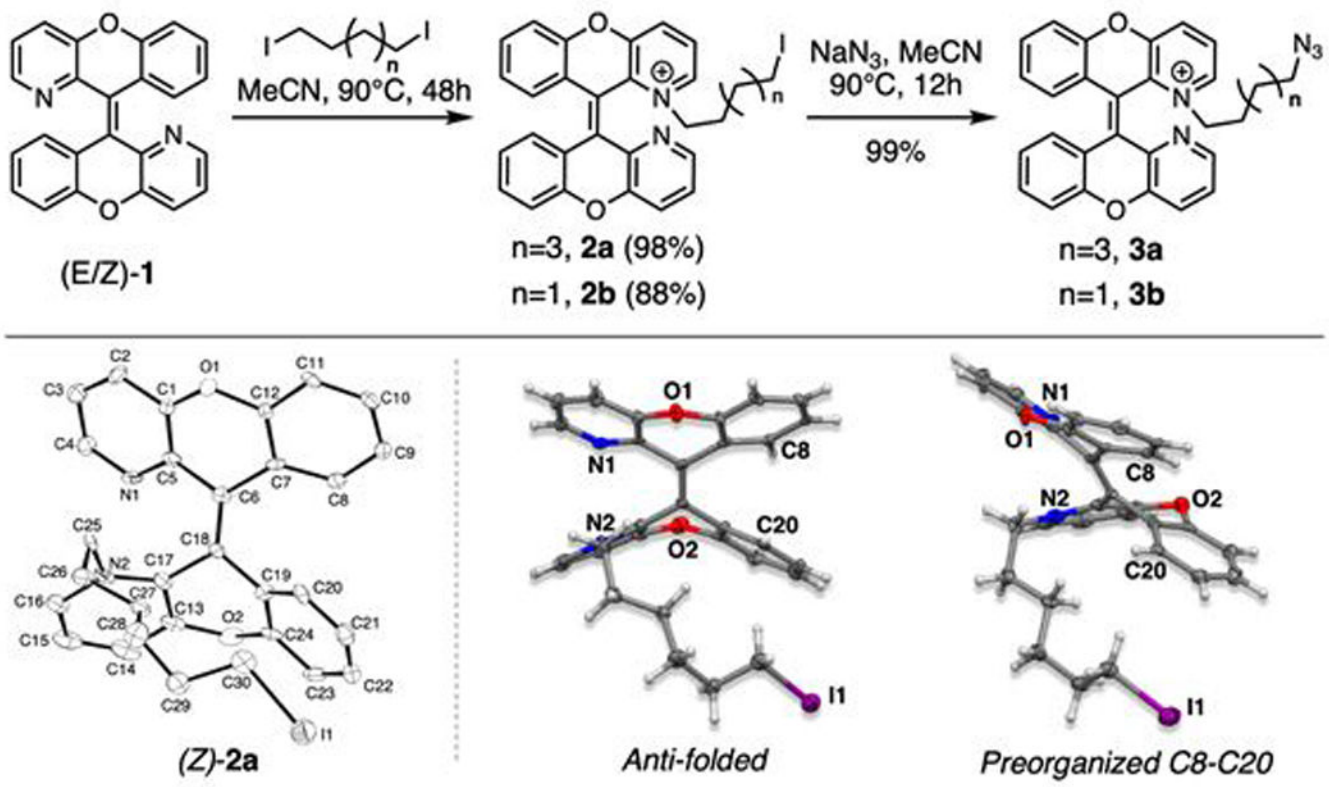

Figure 2.

Schematic reaction for linker synthesis (top) and X-ray crystal structure of anti-folded *(Z)*-**2a** (bottom) are shown.

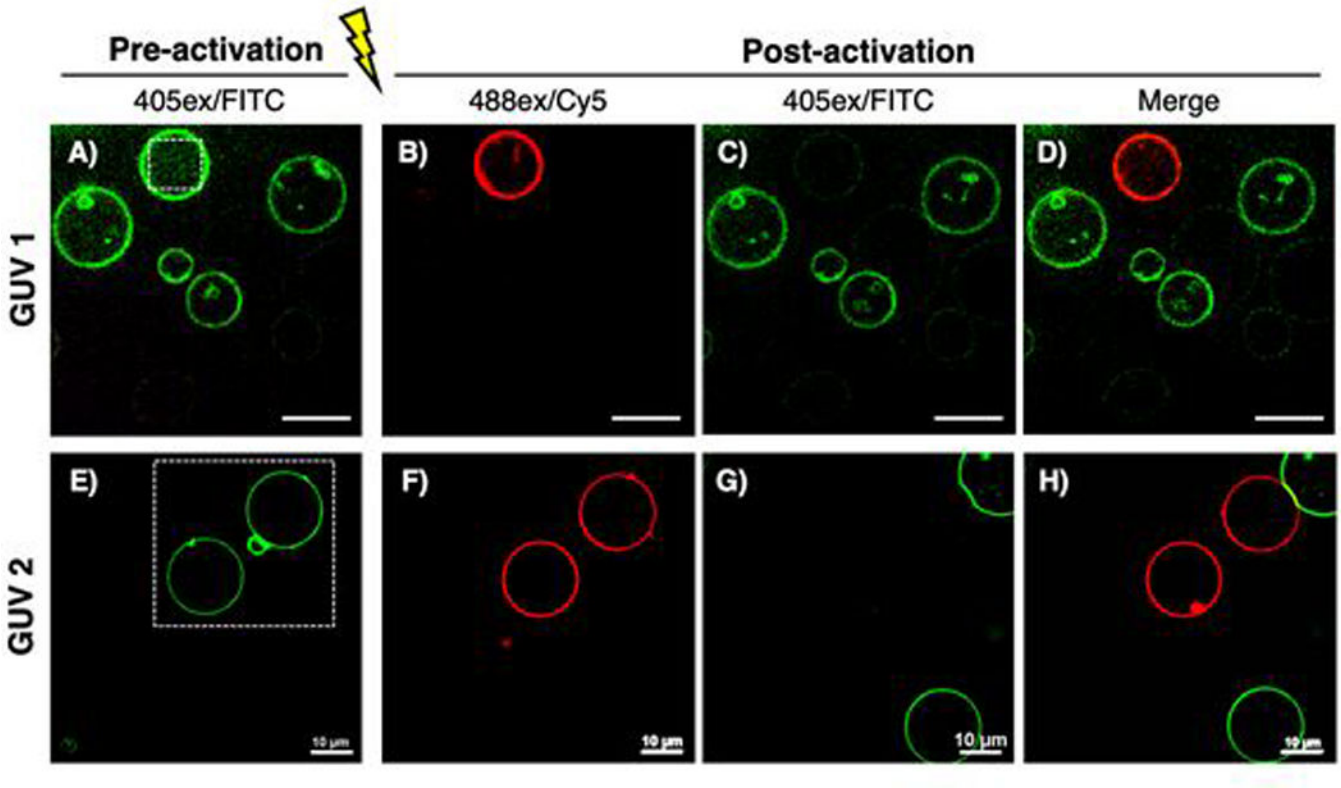

Figure 3.

Photoactivation of **3a** conjugated GUVs. White dotted squares indicate irradiated regions. Pre-activated (A, E) and post-activated (B-D, F-H) GUVs are shown. Images G and H were taken 2 min after photoactivation.

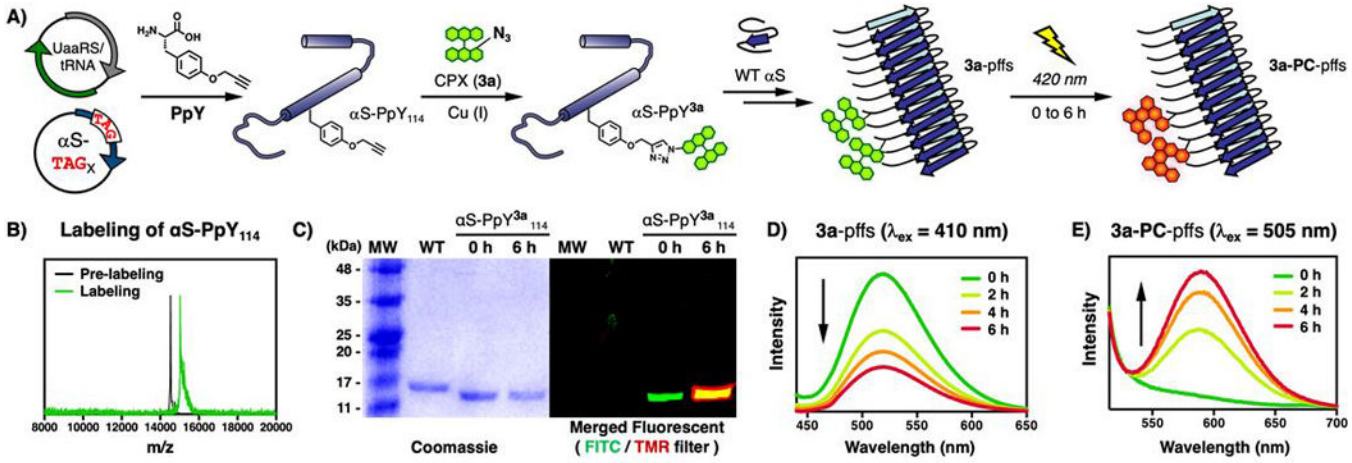

Figure 4.

A) Schematic view of generating **3a**-labeled αS-PpY$_{114}$ pre-formed fibrils (**3a**-pffs) and photoconverted fibrils (**3a-PC**-pffs). B) MALDI-MS and C) SDS-PAGE analysis of wild-type (WT) and **3a**-labeled αS-PpY$_{114}$ (αS-PpY$^{\mathbf{3a}}_{114}$) irradiated for 0 or 6h. FITC (λ_{ex} = 473nm, λ_{em} = 520nm) TMR (λ_{ex} = 532nm, λ_{em} = 580nm) filters are used. D-E) Emission spectra upon photoirradiation to measure disappearance of **3a**-pffs and appearance of **3a-PC**-pffs. PpY is propargyl tyrosine and MW is molecular weight standards.

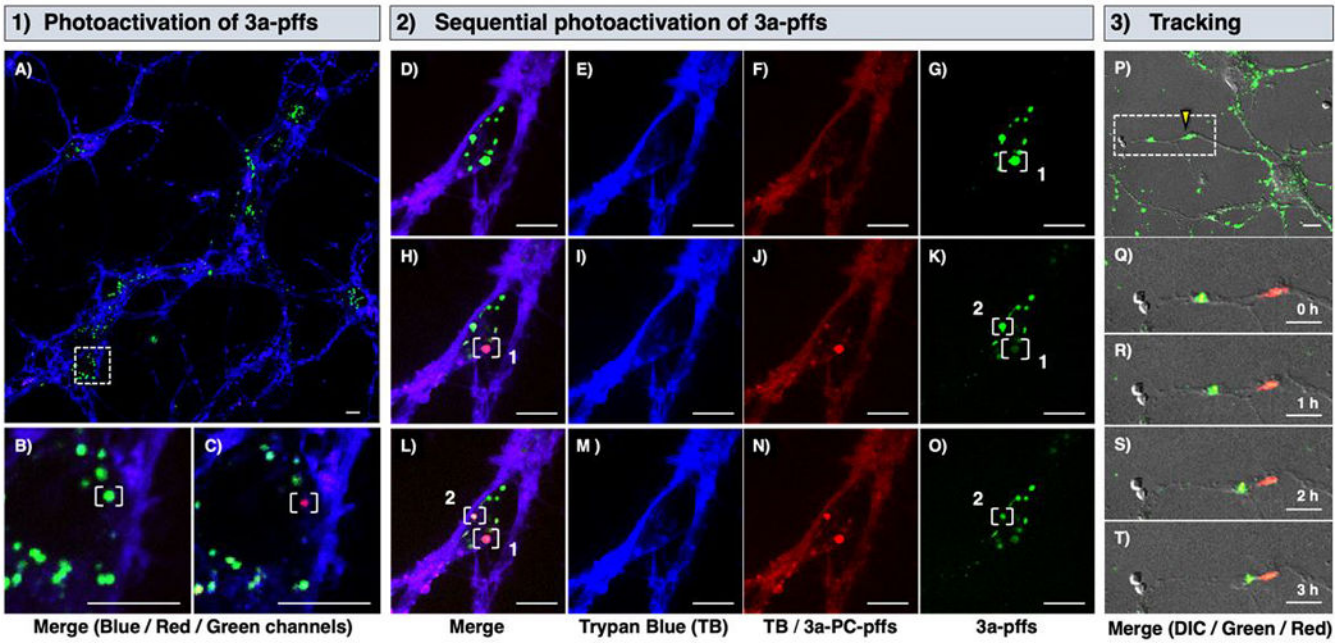

Figure 5.

1) Neuronal uptake and photoactivation of **3a**-pffs. A) Internalized **3a**-pffs (green) in neurons stained with Trypan Blue (blue). White dotted box is zoomed in to show B) pre- and C) post-activation of single endosome/lysosome containing **3a**-pffs in white bracket. 2) Sequential activation of internalized **3a**-pffs in white brackets. Pre-activation (D-G), first post-activation (H-K), and second activation (L-O) are shown in merged, blue (561ex/Cy5), red (488ex/Cy5), and green (488ex/FITC) channels from left to right. 3) Merged images of differential interference contrast (DIC), green and red channels are shown. P) **3a**-pffs under yellow triangle was irradiated and zoomed in (white dotted box) to Q-T) track **3a**-pffs over 3 h. Scale bars are 10 μm. See Supporting Information (S.I.) for details.